doi:10.3788/gzxb20164508.0832001

线性、径向和环向偏振飞秒激光诱导非晶合金周期性表面结构

李晨[1,2],程光华[1]
(1 中国科学院西安光学精密机械研究所 瞬态光学与光子技术国家重点实验室, 西安 710119)
(2 中国科学院大学, 北京 100049)

摘　要:研究在复杂偏振条件下,飞秒激光诱导非晶合金 $Zr_{44}Ti_{11}Cu_{10}Ni_{10}Be_{25}$(at%)表面周期性结构的形成机理.实验采用波长 800 nm、脉宽 120 fs 的超短脉冲激光,分别在线性、径向、环向偏振条件下,诱导非晶合金表面生成复杂的周期性表面结构.表面结构由周期为652～723 nm的低频条纹和周期为1 304～1 765 nm的微型条纹组成.通过有限差分时域法仿真分析,发现微型条纹由粗糙表面引起的定向调制的表面散射电磁波与入射激光干涉形成.仿真结果与实验结果一致,验证了微型条纹形成机理的有效性.

关键词:超快光学;飞秒激光;非晶合金;有限差分时域法;空间光调制器
中图分类号:TG66;O439　　**文献标识码**:A　　**文章编号**:1004-4213(2016)08-0832001-6

Linearly, Radially and Azimuthally Polarized Femtosecond Laser Induced Periodic Surface Structures on Amorphous Alloy

LI Chen[1,2], CHENG Guang-hua[1]
(1 *State Key Laboratory of Transient Optics and Photonics, Xi'an Institute of Optics and Precision Mechanics of CAS, Xi'an* 710119, *China*)
(2 *University of Chinese Academy of Science, Beijing* 10049, *China*)

Abstract: The formation mechanism of Laser Induced Periodic Surface Structures (LIPSS) on the amorphous alloy $Zr_{44}Ti_{11}Cu_{10}Ni_{10}Be_{25}$ (at%) was investigated. In experiment, LIPSS on the amorphous alloy were produced by ultrashort laser pulses of 120 fs duration at 800 nm wavelength in three types of laser polarizations (linear, radial and azimuthal polarization). These LIPSS are comprised of Low-Spatial-Frequency LIPSS (LSFL) with the periodicity of 652～723 nm and macro-ripples with the periodicity of 1 304～1 765 nm. By Finite-Difference Time-Domain (FDTD) simulations, formation mechanism of macro-ripples can be explained by the interference between laser and modulated scattered electromagnetic wave induced by rough surface. In the condition of three types of laser polarizations (linear, radial and azimuthal polarization), FDTD simulation results agree with experimental results, proving the effectiveness of the macro-ripple formation mechanism.

Key words: Laser induced periodic surface structures; Ultrafast laser processing; Amorphous metal; Finite-Difference Time-Domain (FDTD); Spatial Light Modulator (SLM)
OCIS Codes: 320.7130; 320.2250; 160.2750; 140.3300; 140.3390

Foundation item: The National Natural Science Foundation of China (Nos. 61378019, 61223007)
First author: LI Chen (1985－), male, Ph. D. degree candidate, mainly focuses on ultrafast laser machining and measurement. Email: 782969713@qq. com
Supervisor(Corresponding author): CHENG Guang-hua (1976－), male, professor, Ph. D. degree, mainly focuses on ultrafast laser machining. Email: gcheng@opt. ac. cn
Received: Feb. 18, 2016; **Accepted**: Mar. 27, 2016

0 Introduction

Femtosecond (fs) laser has been an excellent and universal tool for micro/nano-fabrication recently. A variety of micro-scale and nano-scale structures can be fabricated in one-step procedure, for example, hole, groove and Laser Induced Periodic Surface Structure (LIPSS)[1-3].

LIPSS is the grating-like damage on the material surface irradiated by laser[4]. Due to its potential application in micro/nano-fabrication, LIPSS has been extensively studied in many kinds of solid materials, such as metals[5], semiconductors[6] and dielectrics[7]. Under the irradiation with multiple linearly polarized fs laser pulses, three types of LIPSS have been observed, such as Low Spatial Frequency LIPSS (LSFL), High Spatial Frequency LIPSS (HSFL) and macro-ripples[4,8-9]. LSFL has a spatial period close to the laser wavelength and LSFL formation mechanism is generally accepted to be the interference of the incident laser with a surface-scattered electromagnetic wave (Sipe theory)[10-11]. HSFL has the spatial periods smaller than the half of laser wavelength[4]. Macro-ripples (or grooves) exhibit the spatial periods in the range of several microns, significantly bigger than laser wavelength[8]. However, the formation mechanisms of HSFL and macro-ripples are still under debate[12-14]. In this work, only LSFL and macro-ripples on amorphous alloy are discussed.

LIPSS has some characteristics, for example, periodicity and orientation. These characteristics can be affected by material properties and fs laser parameters, such as laser polarization, wavelength, fluence, incident angle, pulse duration and pulse number. In particular, complex LIPPS can be made by designed modes of laser polarization, such as radial, azimuthal and other complex vectorial polarizations. Recently, lots of methods have been developed to produce these modes of polarization[15-16]. Among the methods, dynamic programmable liquid-crystal devices are flexible and convenient tools, for example, Spatial Light Modulator (SLM)[17]. In this work, a liquid-crystal SLM is used to convert a linearly polarized fs laser beam to radially or azimuthally polarized vortex beams.

In this work, LIPSS formation mechanism on an amorphous alloy is studied. An amorphous alloy is a solid metallic alloy, with a disordered atomic-scale structure. Due to the lack of crystallites, grain boundaries and dislocations in amorphous structure, amorphous alloy has regular and continuous characteristics in LIPSS and it is helpful to measure the appearance of the LIPSS[9]. Moreover, amorphous alloy is a new functional material and has some advantages of low plastic deformation, low thermal conductivity, high electrical resistance and no defects, so it is useful to research the fs laser micro/nano-fabrication in amorphous alloy. $Zr_{44}Ti_{11}Cu_{10}Ni_{10}Be_{25}$ (at%) is a famous type of amorphous alloys and it has been widely investigated and applied in the industry[18]. So we focus on the LIPSS formation on amorphous alloys $Zr_{44}Ti_{11}Cu_{10}Ni_{10}Be_{25}$.

1 Experiment

The single-side polished Zr-based BMG $Zr_{44}Ti_{11}Cu_{10}Ni_{10}Be_{25}$ (at%) sample with dimensions of 10 mm×6 mm×3 mm is used in the experiment. The sample surface is polished by 0.1 μm polishing fluid. The averaged roughness R_a of the local region on polished surface is about 10 nm, measured by Atomic Force Microscope (AFM). Before and after laser machining, the samples are cleaned ultrasonically in ethanol for 5 min.

A commercial chirped-pulse Ti : sapphire regenerative laser amplifier system (Spitfire, Spectra Physics) is used to generate linearly polarized laser pulses of 120 fs duration at 800 nm wavelength at a pulse repetition frequency of 1 000 Hz. The laser fluence is adjusted by the combination of a wave-plate and a polarizer. Laser pulse energies are measured by an optical power detector. The numbers of pulses are controlled by mechanical shutter. The laser beam is focused by a convex lens with a focus length of 120 mm. The sample is mounted on a computer-controlled translation stage with a spatial resolution of 125 nm and it is observed in the real time by a CCD monitor.

In order to obtain a radial or azimuthal polarized laser beam, the linearly polarized beam is incident through the radial polarization converter (Arcopix Inc.), which is a liquid crystal spatial light modulator. Radially or azimuthally polarized laser emerges on the other side of the radial polarization converter. The switch from radial to azimuthal polarization is controlled by software LC driver (Arcopix Inc.).

Because the ambient air affects the LIPPS formation little, all experiments were carried out in ambient air under normal incidence[19-20]. The surface morphology after fs laser ablation is analyzed with Scanning Electron Microscopy (SEM).

2 Results and analysis

Firstly, linearly polarized fs laser pulses are used to produce LIPSS on amorphous metal. Because LIPSS evolves with the number of laser pulses, the pulse-dependent experiment sare carried out. The morphology of LIPSS on amorphous metal is observed by SEM and the periodicity of ripples is analyzed by two dimensional Fast Fourier Transform (2D-FFT). The results are analyzed as follows.

Fig. 1 shows the SEM images of the LIPSS formed on the amorphous alloy with increasing pulse number (N) by linearly polarized laser at a fixed fluence $\Phi =$ 60 mJ • cm^{-2}. For $N = 1$, there are nano-scale damages and a circle of slight vestige in the irradiated spot, however, LIPSS is not observed [Fig. 1(a)]. For $N=5$, Fig. 1(b) shows that clear LSFL ripples with the orientation perpendicular to the laser polarization are observed in the irradiated spot, which have a quasi-constant periodicity centered at 723 nm. Moreover, faint ripples with direction perpendicular to the laser polarization are also observed, which have a quasi-constant periodicity centered at 1 304 nm, called macro-ripples. Especially, every macro-ripple is comprised of LSFL ripples. After 10 pulses, macro-ripples become clearer with the central periodicity of 1 500 nm, however, LSFL ripples have a smaller central periodicity of 698 nm [Fig. 1(c)]. After 20 pulses, LSFL ripples become weak with the central periodicity of 652 nm and macro-ripples have a central periodicity of 1 765 nm [Fig. 1(d)], which is shown in the space frequency domain by 2D-FFT in Fig. 1(f). As N became 50, the central smooth region without ripples is observed and macro-ripples are only in the annular region, implying that melt and re-solidification took place in the center region [Fig. 1(e)]. This is because that laser beam has Gaussian distribution of fluence in the cross section, the center region in the spot gets the highest energy and firstly starts to melt.

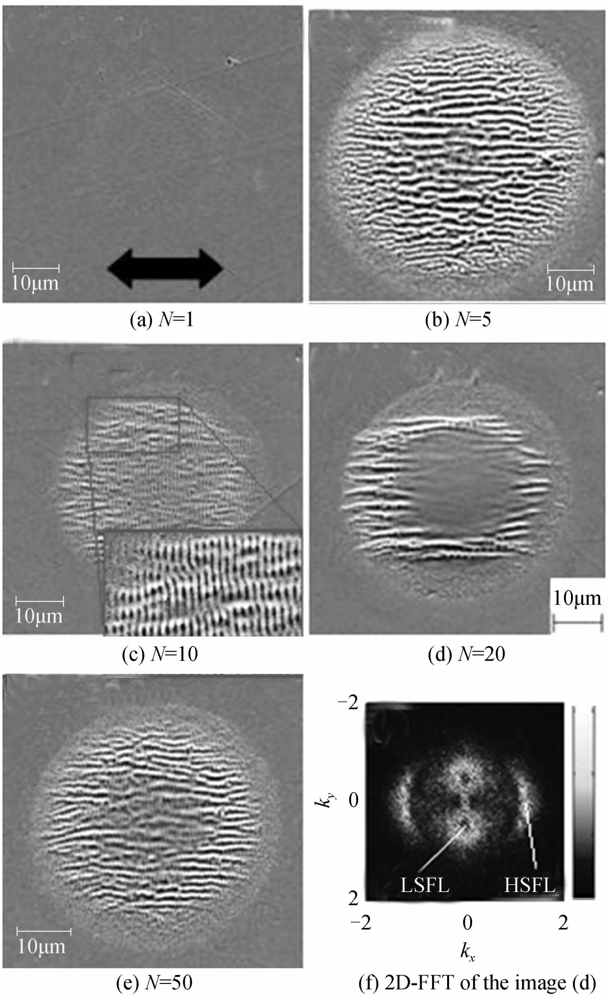

Fig. 1 SEM images of the amorphous metal surface

Next, radially and azimuthally polarized fs laser pulses are used to produce LIPSS on amorphous metal. Fig. 2 shows the SEM images of the amorphous metal surface after irradiation by radially and azimuthally polarized laser at 100 pulses at fluence $\phi = 22.5$ mJ • cm^{-2}. In Fig. 2(a), under radially polarized irradiation, macro-ripples are produced radially and LSFL ripples appear azimuthally around the spot center. In contrast, Fig. 2 (b) shows that macro-ripples are produced azimuthally and LSFL ripples appear radially around the spot center, under azimuthally polarized irradiation.

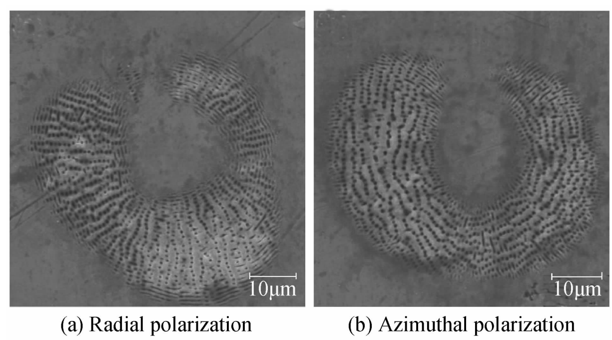

Fig. 2 SEM images of the amorphous metal surface

The initial formation mechanism of LSFL ripples has been investigated in author′s early research work[21]. LIPSS formation is determined by non-homogeneous energy on the surface. After surface nanostructures appear after first laser pulse, the interference between the scattered light and incident laser causes the periodic energy modulation on the surface and contributes to the formation of LSFL ripples. In order to research the formation of macro-ripples, energy modulations on the rough surface induced by linearly, radially and azimuthally polarized laser are investigated by FDTD simulations.

3 FDTD simulations

LIPSS formation is determined by the non-homogeneous absorbed energy on the surface. Non-homogeneous energy modulation is mainly from the interference between incident laser and scattered electromagnetic wave induced by nano-structures on surface. In this article, Finite-Difference Time-Domain (FDTD) method is used to compute the energy distribution of electric field on the surface. FDTD method can simulate light propagation, scattering and diffraction by solving Maxwell′s equations numerically, which was introduced by Yee in 1966[10-11]. This method has been a powerful engineering tool for integrated and diffractive optics device simulations.

In FDTD simulation, amorphous metal is irradiated at normal in air with a laser pulse of 120 fs duration at 800 nm wavelength. The refractive index of amorphous metal is $\tilde{n}=2.274+3.337i$, measured by spectroscopic phase modulated ellipsometer (Uvisel, Horiba Jobin Yvon). Perfect Match Layer (PML) is used as boundary conditions.

3.1 LIPSS formation on rough surface induced by linearly polarized laser

In order to research LIPSS formation on rough surface, the flat surface with 1000 cubic nano-particles in random distribution is built as FDTD model. Single cubic particle size is 40 nm×40 nm×40 nm. The surface size is 25 μm×25 μm and 20% of the area is filled with the cubic particles. The incident plane wave propagates along the Z axis, representing the incident laser. The plane wave has the 800 nm wavelength and its polarization is along X axis with the electric field amplitude of 1 V/m. Because the polarization of incident plane wave is defined along E_x, new developed electric field E_z components only include the scattered field. FDTD simulation is carried out and results are shown in Fig. 3.

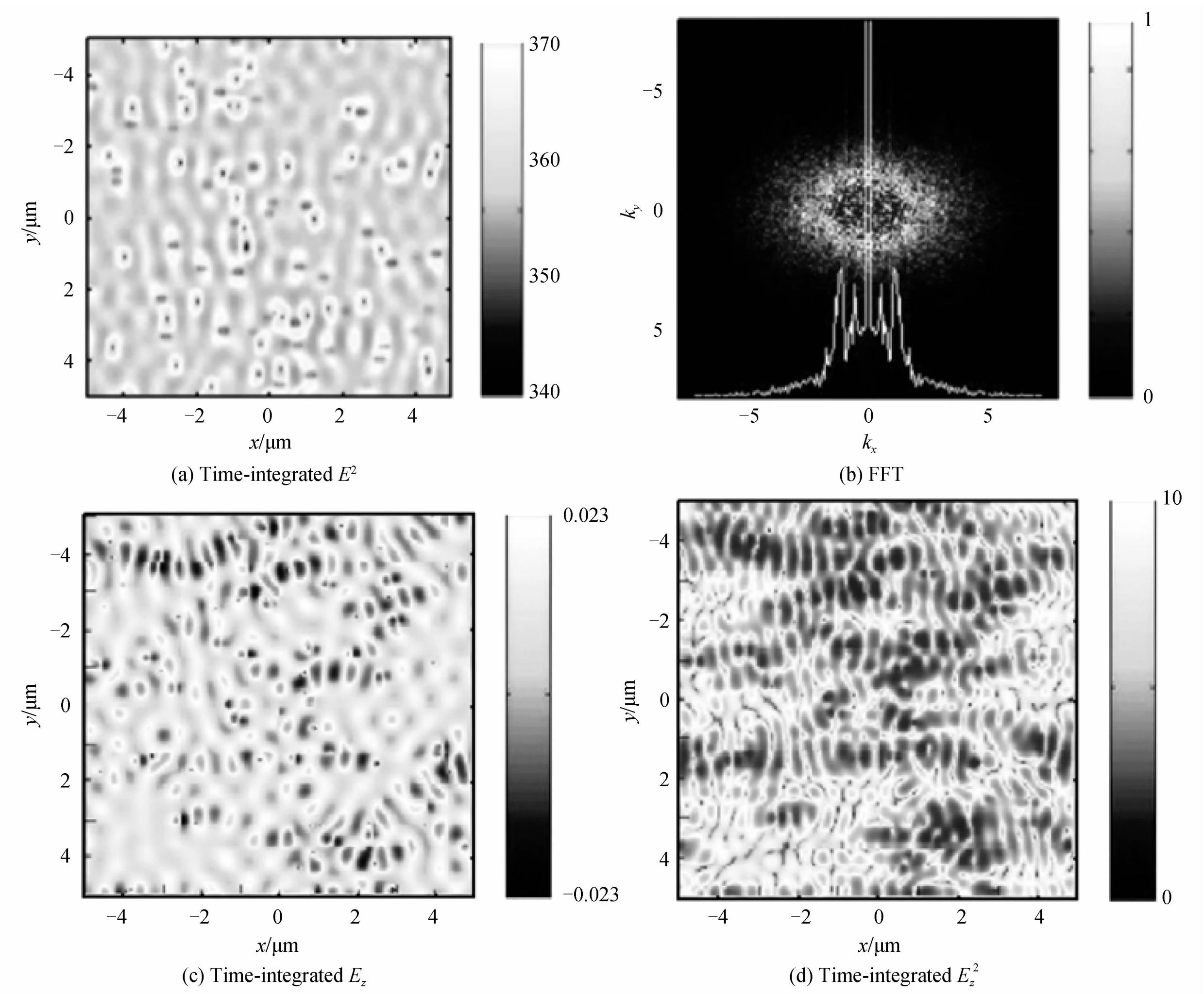

Fig. 3 Time-averaged distribution on the rough surface and the corresponding FFT image

Fig. 3(a) is the time-averaged E^2 for one pulse duration on rough surface, which shows a stationary spatially modulated energy pattern like LSFL ripples. Fig. 3(b) is the 2D-FFT of Fig. 3(a), showing that energy modulation pattern has the center space period of 769.2 nm with the direction perpendicular to the laser polarization. This energy modulation pattern is mainly from the interference between incident plane wave and scattered electromagnetic wave induced by the nano-particles on surface. So the formation of LSFL ripples can be explained by the interference between the scattered electromagnetic wave and incident laser[19].

The orientation of LSFL is determined by laser polarization, not affected by surface roughness. The spatial periods of LSFL are affected a little by surface roughness, because LIPSS formations are determined by the interference between incident laser and surface scattered wave, and the periods of surface scattered wave are affected a little by the nanoparticle size and the number of particles in the rough surface [22].

Fig. 3(c) is the electric field E_z nearly on the same rough surface in one moment, which shows that the directed scattered electromagnetic wave along X axis induced by multiple nano-particles propagates almost along the polarization. The directed scattered electromagnetic wave interferes with incident planewave, contributing to the macro-ripple formation.

Fig. 3(d) is the time-averaged E_z^2 for one pulse duration on same rough surface, which shows a stationary spatially modulated energy pattern almost along the polarization, related to the macro-ripple formation. So the formation of macro-ripples on rough surface can be explained by the interference between laser and directed scattered electromagnetic wave induced by rough surface.

3.2 LIPSS formation on rough surface induced by radially and azimuthally polarized laser

In order to research LIPSS formation on rough surface induced by radially and azimuthally polarized laser, the same rough surface model in Fig. 3 is used in this simulation. The incident 6-order Gaussian laser beam with radial or azimuthal polarization propagates in the Z axis. In the same simulation condition in Fig. 3, FDTD simulations are carried out and results are shown in Fig. 4.

Fig. 4(a) is the electric field E_z nearly on the rough surface induced by radially polarized laser in one moment, which shows that the radially modulated scattered electromagnetic wave induced by rough surface propagates almost along the polarization. According to the conclusion in Fig. 3, the radially modulated scattered electromagnetic wave interferes with incident laser, contributing to the macro-ripple formation in radial direction, which is consistent with experiment result in Fig. 2(a). In comparison, Fig. 4(b) is the electric field E_z nearly on the rough surface induced by azimuthally polarized laser in one moment, which shows the azimuthally modulated scattered electromagnetic wave. Moreover, the azimuthally modulated scattered electromagnetic wave interferes with incident laser, contributing to the macro-ripple formation in azimuthal direction, which is consistent with experiment result in Fig. 2(b).

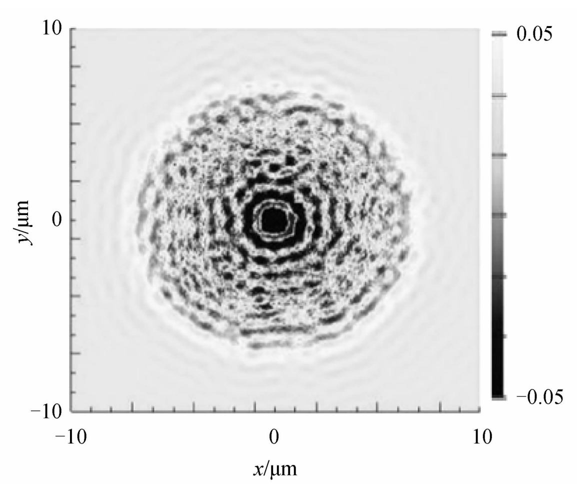

(a) E_z distribution induced by radially polarized laser

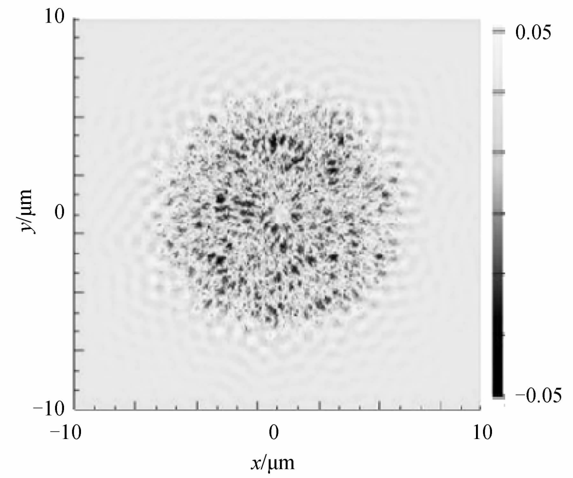

(b) E_z distribution induced by azimuthally polarized laser

Fig. 4 Electric field distribution on the surface

In total, LIPSS formation on rough surface induced by linearly, radially and azimuthally polarized laser can be explained by the interference between laser and modulated scattered electromagnetic wave induced by rough surface.

4 Conclusion

The fs-LIPSS formations on amorphous alloy $Zr_{44}Ti_{11}Cu_{10}Ni_{10}Be_{25}$ (at%) upon normal irradiation with linearly, radially and azimuthally polarized laser pulses of 120 fs duration at 800 nm wavelength are investigated in the experiments. Two distinct types of fs-LIPSS: LSFL ripple and macro-ripple are observed in experimental results. LSFL ripples perpendicular to the laser polarization have the periodicity of 652 nm～723 nm. Macro-ripples parallel to the laser polarization have the periodicity of 1 304 nm ～ 1 765 nm, especially, every macro-ripple is comprised of LSFL ripples. The laser polarization is controlled by spatial light modulator. Under the irradiation of radial or azimuthal polarization, LIPSS shows the complex structures. LIPSS formations on rough surface induced by linearly, radially and azimuthally polarized laser are investigated by FDTD simulations. LIPSS formation can be explained by the interference between laser and modulated scattered electromagnetic wave induced by rough surface. FDTD simulation results agree with experimental results.

References

[1] BUIVIDAS R, MIKUTIS M, JUODKAZIS S. Surface and bulk structuring of materials by ripples with long and short laser pulses: recent advances[J]. *Progress in Quantum Electronics*, 2014, **38**(3): 119-156.

[2] WANG F, LUO J, LI M. High-precidion method of machining taper holes of diesel engine nozzle with femtosecond laser[J]. *Acta Photonica Sinica*, 2014, **43**(4): 0414003.

[3] YAO H, YU W, YANG Z, *et al*. Numerical simulation of AZ31B magnesium alloy shocked with femtosecond laser[J]. *Acta Photonica Sinica*, 2015, **44**(4): 0414002.

[4] BONSE J, KRUGER J. Femtosecond laser-induced periodic surface structures[J]. *Journal Laser Applications*, 2012, **24**(4): 042006.

[5] BIZI-BANDOKI P, VALETTE S. Effect of stationary femtosecond laser irradiation on substructures formation on a mold stainless steel surface[J]. *Applied Surface Science*, 2013, **270**: 197-204.

[6] SKOLSKI J Z P, RÖMER GR B E, *et al*. Laser-induced periodic surface structures: Fingerprints of light localization [J]. *Physical Review B*, 2012, **85**(7): 3711-3711.

[7] HÖHM S, ROSENFELD A. Femtosecond laser-induced periodic surface structures on silica[J]. *Journal Applied Physics*, 2012, **112**(1): 014901.

[8] REIF J, MARTENS C, UHLIG S, *et al*. On large area LIPSS coverage by multiple pulses[J]. *Applied Surface Science*, 2015, **336**: 249-254.

[9] ZHANG W, CHENG G, HUI X D, *et al*. Abnormal ripple patterns with enhanced regularity and continuity in a bulk metallic glass induced by femtosecond laser irradiation[J]. *Applied Physics A*, 2014, **115**(4): 1451-1455.

[10] SIPE J E, YOUNG J F, PRESTON J S, *et al*. Laser-induced periodic surface structure. I. theory[J]. *Physical Review B*, 1983, **27**(2): 1141-1154.

[11] BONSE J, ROSENFELD A, KRÜGER J. Implications of transient changes of optical and surface properties of solids during femtosecond laser pulse irradiation to the formation of laser-induced periodic surface structures[J]. *Applied Surface Science*, 2011, **257**(12): 5420-5423.

[12] NATHALA C S R, AJAMI A, IONIN A A, *et al*. Experimental study of fs-laser induced sub-100-nm periodic surface structures on titanium[J]. *Optics Express*, 2015, **23**(5): 5916-5929.

[13] LI X F, ZHANG C Y, LI H, *et al*. Formation of 100-nm periodic structures on a titanium surface by exploiting the oxidation and third harmonic generation induced by femtosecond laser pulses[J]. *Optics Express*, 2014, **22**(23): 28086-28099.

[14] ZHANG W, CHENG G. Abrupt transition from wavelength structure to subwavelength structure in a single-crystal superalloy induced by femtosecond laser[J]. *Applied Surface Science*, 2011, **257**: 4321-4324.

[15] HNATOVSKY C, SHVEDOV V, KROLIKOWSKI W, *et al*. Revealing local field structure of focused ultrashort pulses [J]. *Physical Review Letters*, 2011, **106**(12): 123901.

[16] BASHKANSKY M, PARK D, FATEMI F K. Azimuthally and radially polarized light with a nematic SLM[J]. *Optics Express*, 2010, **18**(1): 212-217.

[17] ALLEGRE O J, PERRIE W, EDWARDSON S P. Laser microprocessing of steel with radially and azimuthally polarized femtosecond vortex pulses[J]. *Journal of Optics*, 2012, **14**(8): 085601.

[18] SCHROERS J, NGUYEN T, O' KEEFFE S, *et al*. Thermoplastic forming of bulk metallic glass-applications for MEMS and microstructure fabrication[J]. *Materials Science and Engineering*: *A*, 2007, **449**(13): 898-902.

[19] KALSOOM U, BASGUR S. Effect of ambient environment on excimer laser induced micro and nano-structuring of stainless steel[J]. *Applied Surface Science*, 2012, **261**: 101-109.

[20] YAMAGUCHI M, UENO S. Raman spectroscopic study of femtosecond laser-induced phase transformation associated with ripple formation on single-crystal SiC[J]. *Applied Physics A*, 2010, **99**(1): 23-27.

[21] LI C, CHENG G, COLOMBIER J P, *et al*. Impact of evolving surface nanoscale topologies in femtosecond laser structuring of Ni-based superalloy CMSX-4[J]. *Journal of Optics*, 2016, **18**(1): 015402.

[22] LI C, CHENG G, STOIAN R. Investigation of femtosecond laser-induced periodic surface structures on tungsten[J]. *Acta Optica Sinica*, 2016, **36**(5): 053200.

[23] LEVEQUE G, MARTIN O J F. Transient behavior of surface plasmon polaritons scattered at a subwavelength groove[J]. *Physical Review B*, 2007, **76**(76): 155418.